A MODEL FOR THE THERMAL RADIO CONTINUUM EMISSION PRODUCED BY A SHOCK WAVE AND ITS APPLICATION TO THE HERBIG-HARO OBJECTS 1 AND 2

Salvador Curiel, Jorge Cantó y Luis F. Rodríguez

Instituto de Astronomía
Universidad Nacional Autónoma de México

RESUMEN. Se presenta un modelo para la estimación del continuo térmico en radio producido por una onda de choque y su aplicación a las observaciones en 20, 6 y 2 cm del sistema HH 1-2 (Pravdo et al. 1985). Esta es la primera vez que se lleva a cabo este tipo de cálculo. El espectro obtenido, muy similar al observado en regiones HII, reproduce satisfactoriamente el espectro observado en los objetos HH1 y 2, mientras que en el caso de la fuente central (posible fuente excitadora de dichos objetos), el espectro observado sólo puede ser reproducido parcialmente. Estos resultados pueden deberse a que la emisión en radio de la fuente central no sea producida por una onda de choque como tal, sino por otro fenómeno distinto, como podría ser un viento estelar ionizado e isotérmico o posiblemente, por una combinación de ambos. Aún cuando el espectro de continuo térmico de radio producido por una onda de choque es muy similar al de una región fotoionizada, existen dos diferencias significativas en la parte ópticamente gruesa: 1) la temperatura de brillo de una región ionizada por choque puede exceder considerablemente el valor máximo de $\sim 10^4$ K esperado para una región HII, y 2) el índice espectral de una región ionizada por choque puede exceder el valor máximo de 2 esperado para una región HII.

ABSTRACT. We present a model for the thermal radio continuum emission produced by a shock wave and its application to the observations at 20, 6 and 2 cm of the HH1-2 system (Pravdo et al. 1985). This is the first time that this type of calculation is made. The obtained spectrum, very similar to that observed in HII regions, can reproduce satisfactorily the observed spectra in HH1 and 2, while in the case of the central source (possibly the exciting source of these HH objects), the observed spectrum can be reproduced only partially. These results suggest that the radio emission of the central source is not produced by a shock wave but by a different phenomenon such as an isothermal, ionized stellar wind or possibly a combination of both phenomena. Although the thermal radio continuum spectrum produced by a shock wave is very similar to that from a photoionized region, there are two significant differences in the optically thick part: 1) the brightness temperature from a shock-ionized region can exceed considerably the maximum value of $\sim 10^4$ K expected for an HII region, and 2) the spectral index from a shock-ionized region can exceed the maximum value of 2 expected for an HII region.

Key words: HERBIG-HARO OBJECTS — RADIO CONTINUUM

I. INTRODUCTION

The Herbig-Haro (HH) objects 1 and 2 were discovered independently by Herbig (1951) and Haro (1952) in the vicinity of the reflection nebula NGC1999. They were the first objects of their class reported and since then they have been the subject of extensive studies from radio to X-ray frequencies.

The HH objects are formed by compact condensations of semistellar appearance that exhibit an emission spectrum dominated by lines from low excitation species such as OI, SII and NII, as well as hydrogen lines. The similarity between the HH spectra and those observed in low velocity supernova remnants, in addition to the highly supersonic motions that they possess, suggest that HH objects are the product of a shock wave, probably produced by the wind of a young star. Raymond (1976, 1979), Dopita (1978), and Shull and McKee (1979) made detailed calculations of the emission spectra of a steady state, plane-parallel shock wave and showed that in general the visible spectrum of HH objects can be reproduced with preshock densities of ~100 cm^{-3} and shock velocities of ~100 km s^{-1}. However, the UV spectra of HH1 and 2 (Böhm 1983) show emission lines of high excitation ions (CIII, CIV, OIII, OIV, SiIII and SiIV) whose intensities can not be reproduced with the same shock wave model that explains the visible spectrum. The high excitation UV lines suggest a larger shock wave velocity (~200 km s^{-1}). A possible explanation for this apparent discrepancy is that the HH objects are the result of bow shocks, produced by the interaction of small condensations with a less dense, supersonic flow (Schwartz 1978; Hartmann and Raymond 1984). In this case, the observed spectrum is a combination of spectra produced by a continuum of shock waves with velocities from that of the flow to much smaller values.

Hartmann and Raymond (1984) presented detailed calculations of bow shock waves with maximum velocities in the 160 to 300 km s^{-1} range. They found that the line widths and the visible and UV spectra of HH1 and 2 agree reasonably with the theoretical calculations for a shock velocity of ~200 km s^{-1}. Since these velocities are comparable with the velocities of HH1 and 2 (Herbig and Jones 1981), they concluded that these HH objects are condensations moving super--sonically in a less dense medium.

Pravdo et al. (1985) detected for the first time radio continuum emission from HH1 and 2 at 20, 6 and 2 cm. They also detected emission from a source located midway between HH1 and 2 (the so-called central source). From the analysis of their data, they found spectral indices of -0.2±0.3 for HH1 and of -0.2±0.1 for HH2. This result suggests that for these objects the emission mechanism is optically-thin free-free radiation. On the other hand, the central source has a spectral index of 0.4±0.2, marginally consistent with the value of 0.6 expected for an isothermal, ionized stellar wind (Wright and Barlow 1975; Panagia and Felli 1975).

In this paper we present a model for the thermal radio continuum emission produced by a shock wave and its application to the HH1 and 2 observations of Pravdo et al. (1985). In § II we calculated analytically the Hβ and thermal radio continuum emission produced in the recombination zone of a shock wave. We also calculate numerically the thermal radio continuum emission from the complete shock wave (cooling zone plus recombination zone). In §III we discuss the model and present its results, while in §IV we apply it to the radio observations of HH1 and 2. Finally, in §V we give our conclusions.

II. THE MODEL

a) Hβ Emission from the Recombination Zone.

In the recombination zone the electron temperature is low enough (~10^4 K) to neglect collisional excitation for hydrogen, and consequently Hβ is produced mainly by recombination. For a plane-parallel shock wave, the Hβ intensity (produced in a volume V_R with depth D_r and transverse area of 1 cm^2) is given by

$$I(H_\beta) = \int_0^{D_r} j_{H\beta} \, dr = a(T) \, E_m \qquad \text{erg cm}^{-2} \text{ s}^{-1} \text{ str}^{-1}, \qquad (1)$$

we $j_{H\beta} = a(T) \, n_e n_p$ is the Hβ emission coefficient, n_e and n_p are the number density of electrons and protons, and E_m is the emission measure.

On the other hand, the recombination rate, N_R, for the volume V_R is:

$$N_R = \int_0^{D_r} \alpha_B \, n_e \, n_p \, dr = \alpha_B \, E_m \, , \qquad (2)$$

were α_B is the total recombination coefficient (excluding recombinations to the ground level).

Furthermore, N_R also equals the number of ionized atoms that enter the recombination zone per second per cm^2, $n_o v_o X^*$, minus the number of ionized atoms that leave the recombination zone per second per cm^2, $n_o v_o X_f$, plus the photoionization rate per cm^2 produced in the recombination zone by photons from the cooling zone, $n_o v_o \Phi$. Thus,

$$N_R = n_o v_o [X^* - X_f + \Phi] \quad , \tag{3}$$

were n_o is the preshock density, v_o is the shock velocity, X^* is the fraction of ionized atoms that enter the recombination zone, X_f is the fraction of ionized atoms that leave the recombination zone, and Φ is the number of ionizing photons produced per atom, that enter the shock wave (we have assumed that each one of these photons ionizes only one hydrogen atom).

Combining equations (2) and (3) we find that the emission measure is given by:

$$E_m = \frac{n_o v_o}{\alpha_B} [X^* - X_f + \Phi] \quad , \tag{4}$$

and if we substitute this formula in equation (1) we obtain that the Hβ intensity from the recombination zone is:

$$I(H_\beta) = n_o v_o \frac{a(T)}{\alpha_B} [X^* - X_f + \Phi] \quad . \tag{5}$$

Following Osterbrock (1974), $a(T) = 9.86 \times 10^{-27} T_4^{-0.8}$ erg cm^3 s^{-1} str^{-1} (case B) and $\alpha_B = 2.6 \times 10^{-13} T_4^{-0.8}$ cm^3 s^{-1}, were T_4 is the electron temperature in units of 10^4 K. Furthermore, from Curiel (1986), $\Phi = 3.48 v_7 - 2.745$ (where $v_7 = v_o / 100$ km s^{-1}), $X_f = 1.0 \times 10^{-2}$ and X^* is of order unity for $v_7 \geq 2$. The Hβ intensity can then be written as:

$$I(H_\beta) = 3.795 \times 10^{-6} \left[\frac{n_o}{10 \ cm^{-3}} \right] \left[\frac{v_o}{100 \ km \ s^{-1}} \right] [(3.483 v_7 - 2.745) + (X^* - X_f)] \quad . \tag{6}$$

b) Thermal Radio Continuum from the Recombination Zone.

In this work we will consider only shock waves with $v_o \sim 200$ km s^{-1} and weak magnetic fields ($\sim$tens of μGauss). In this case, we expect that the radio continuum emission will be of free-free type (also called thermal or bremsstrahlung). For a plane-parallel shock wave with an approximately isothermal ($\sim 10^4$ K) recombination zone, the intensity will be given by:

$$I_\nu = F_\nu (1 - e^{-\tau_\nu}) \quad , \tag{7}$$

where F_ν is the source function and τ_ν is the optical depth at frequency ν, which is defined by:

$$\tau_\nu = \int_0^{D_r} n_e n_p \chi(\nu) \ dr = \chi(\nu) E_m \quad , \tag{8}$$

where $\chi(\nu) = 8.436 \times 10^{-28} \left[\frac{\nu}{10 \ GHz} \right]^{-2.1} \left[\frac{T_e}{10^4 \ K} \right]^{-1.35} \tag{9}$

in the radio wavelengths (Mezger and Henderson 1967). For a system in thermal equilibrium:

$$F_\nu = B_\nu(T_e) = \frac{2h\nu^3/c^2}{\exp(h\nu/kT_e) - 1} \quad . \tag{10}$$

Equation (7) has two limit cases:

$$I_\nu \approx B_\nu(T_e)\tau_\nu \; ; \quad \text{for } \tau_\nu \ll 1, \tag{11}$$

and

$$I_\nu \approx B_\nu(T_e) \; ; \quad \text{for } \tau_\nu \gg 1. \tag{12}$$

Assuming that the Rayleigh-Jeans approximation is valid, equations (11) and (12) become

$$I_\nu \approx \frac{2\nu^2 k T_e}{c^2}\tau_\nu = 2.587\times10^{-40}\left[\frac{\nu}{10\text{ GHz}}\right]^{-0.1}\left[\frac{T_e}{10^4\text{ K}}\right]^{-0.35} E_m \tag{13}$$

and

$$I_\nu \approx \frac{2\nu^2 k T_e}{c^2} = 3.067\times10^{-13}\left[\frac{\nu}{10\text{ GHz}}\right]^{2}\left[\frac{T_e}{10^4\text{ K}}\right] , \tag{14}$$

respectively. Substituting equation (4) in equation (13) we obtain a formula for I_ν when $\tau \ll 1$ in terms of the shock parameters, i. e.,

$$I_\nu \approx 9.95\times10^{-20}\left[\frac{\nu}{10\text{ GHz}}\right]^{-0.1}\left[\frac{T_e}{10^4\text{ K}}\right]^{0.45}$$

$$\times \left[\frac{n_o}{10\text{ cm}^{-3}}\right]\left[\frac{v_o}{100\text{ km s}^{-1}}\right][X^* - X_f + \Phi] . \tag{15}$$

c) Correlation between I_ν and $I(H\beta)$.

In the optically thin region we obtain from equations (1) and (13)

$$\frac{I_\nu}{I(H_\beta)} = 2.62\times10^{-14}\left[\frac{\nu}{10\text{ GHz}}\right]^{-0.1}\left[\frac{T_e}{10^4\text{ K}}\right]^{0.45} . \tag{16}$$

This ratio is independent of the shock parameters and depends only on the electron temperature and, very weakly, on the frequency.

d) Numerical Solution for I_ν and $I(H\beta)$.

To determine more accurately the intensity of radiation of the emission from a shock wave it is necessary to consider the radiation transfer across the shock wave. For a plane-parallel geometry, the transfer equations of $I(H\beta)$ and I_ν are

$$\frac{d I(H\beta)}{dr} = j_{H\beta} , \quad \text{and} \tag{17}$$

$$\frac{dI_\nu}{dr} = \kappa_\nu [F_\nu - I_\nu] , \tag{18}$$

where the absorption coefficient, κ_ν, is given in the radio by

$$\kappa_\nu = 3.69\times10^8\, n_e n_p \nu^{-3} T_e^{-\frac{1}{2}}(1-e^{-h\nu/kT_e})g_{ff} \quad \text{cm}^{-1} \tag{19}$$

and the Gaunt factor is

$$g_{ff} = 9.77 \left[1 + 0.131 \log \frac{T_e^{3/2}}{\nu} \right]$$ (20)

    In the case of Hβ the radiation travels across the shock wave without being absorbed. Equations (17) and (18) together with equations for the fraction of ionized gas and for the flux of ionizing photons at each point of the shock wave form a system of coupled differential equations that can be solved only numerically. We integrated this system of equations using the Runge-Kutta method of fourth order for simultaneous differential equations (Abramowitz and Stegun 1972). To carry on this integration we used the shock wave structure of Curiel (1986). In this numerical integration the cooling zone and the recombination zone are taken into account. As we will see in §III, the numerical results for the complete shock wave (cooling zone plus recombination zone) are similar to those obtained analytically considering only the recombination zone.

III. DISCUSSION

    Equation (6) gives the Hβ intensity as a function of the shock parameters. As can be seen in that equation and in Figure 1, for velocities larger than 130 km s^{-1}, the Hβ intensity grows approximately as $n_o v_o^2$, a result in agreement with those obtained by Raymond (1976, 1979) and Shull and McKee (1979). Also, from equations (14) and (15) and from Figure 2, it is evident that the radio continuum spectrum calculated analytically for the shock wave is similar to those observed in H II regions. This is, of course, as expected because in the analytical solution we consider only an isothermal zone. For the numerical solution, however, there are significant differences in the calculated radio continuum spectrum with respect to that from an H II region. The main reason for these differences is that the numerical solution takes into account the cooling zone, which has an electron temperature much larger than 10^4K.

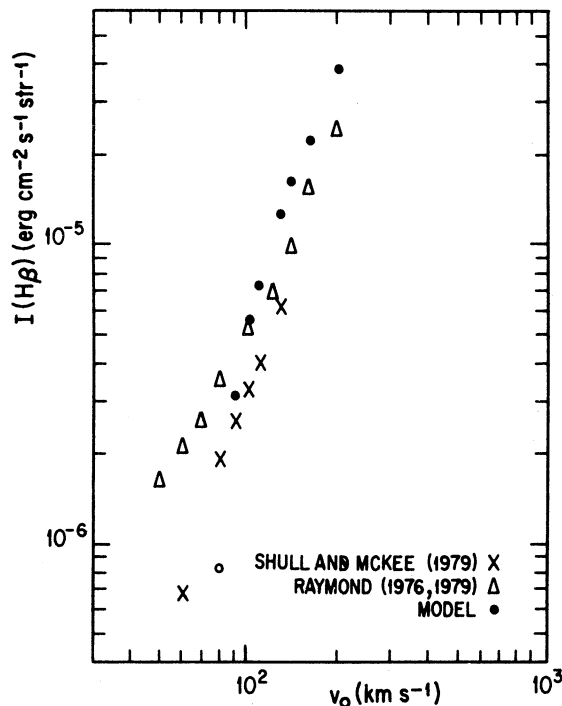Fig. 1. Hβ intensity as a function of shock velocity for several shock wave models. In all cases $n_0 = 10$ cm^{-3} and $B_0 = 1$ μGauss. Note the reasonable agreement between the models for $v_0 \geq 130$ km s^{-1}.

We have calculated the radio continuum spectrum for a shock wave along a line of sight perpendicular to the shock wave front both for the case where the observer is on the side of the recombination zone (case I) as when the observer is on the side of the cooling zone (case II). Since the shock wave is not symmetric, differences appear (Figure 2). The most obvious difference is that at large optical depths (low frequencies) in case I a brightness tempera-- ture of 10^4 K is determined, while larger values appear for case II. In case I there is a small part of the spectrum where the spectral index exceeds the value of 2. Unfortunately, these effects appear at very low frequencies that at present are difficult to observe. On the other hand, at high frequencies cases I and II give the same result and agree as well with the analy-- tical solution. Since the observations of Pravdo et al. (1985) are in the optically thin part of the spectrum, we will interpret them using the analytical solution.
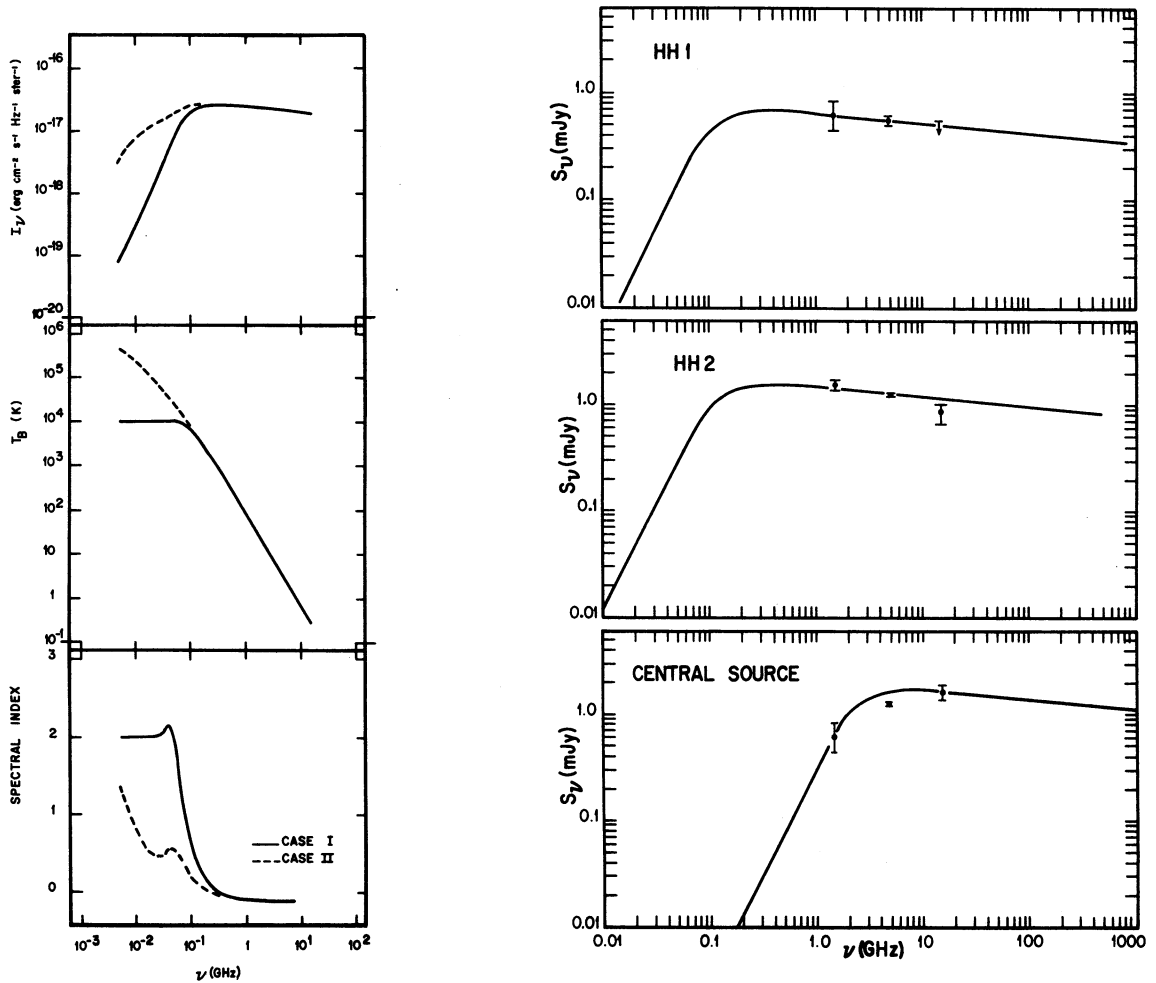

Fig. 2. Radio continuum spectrum (top), brightness temperature (middle), and spectral index (bottom) from the numerical model with $n_0 = 100$ cm^{-3}, $v_0 = 200$ km s^{-1} and $B_0 = 1$ μGauss. The results for the cases I and II (see text) are shown.

Fig. 3. Fits of the analytical model to the Pravdo et al. (1985) data of HH1, HH2 and the Central Source. The shock parameters are given in Table 1.

IV. APLICATION OF THE ANALYTICAL MODEL TO THE RADIO OBSERVATIONS OF HH1 AND 2.

To apply the model to the radio observations we note that the $H\beta$ and radio con-tinuum fluxes are given by:

and

$$F(H_\beta) = I(H_\beta) \, \Omega \approx (\pi/4)I(H_\beta)\Theta^2 \quad , \tag{21}$$

$$S_\nu = I_\nu\Omega \approx (\pi/4)I_\nu \Theta^2 \quad , \tag{22}$$

where Ω is the solid angle of the source (assumed to be a disk) and Θ is the source angular diameter in radians. From equation (16), (21) and (22) we obtain:

$$\left[\frac{S_\nu}{mJy}\right] = 2.62\times10^{12}\left[\frac{\nu}{10 \text{ GHz}}\right]^{-0.1}\left[\frac{T_e}{10^4 \text{ K}}\right]^{0.45}\left[\frac{F(H_\beta)}{\text{erg cm}^{-2} \text{ s}^{-1}}\right] \quad , \tag{23}$$

and from equations (14), (15) and (22) we obtain two equations for the radio flux, the first for $\tau_\nu \gg 1$;

$$\left[\frac{S_\nu}{mJy}\right] = 5.66\times10^2\left[\frac{\nu}{10 \text{ GHz}}\right]^2\left[\frac{\Theta}{\text{arc sec}}\right]^2\left[\frac{T_e}{10^4 \text{ K}}\right] \quad ; \tag{24}$$

and the second for $\tau_\nu \ll 1$;

$$\left[\frac{S_\nu}{mJy}\right] = 1.84\times10^{-4}\left[\frac{\nu}{10 \text{ GHz}}\right]^{-0.1}\left[\frac{\Theta}{\text{arc sec}}\right]^2\left[\frac{T_e}{10^4 \text{ K}}\right]^{0.45}$$

$$\times \left[\frac{n_o}{10 \text{ cm}^{-3}}\right]\left[\frac{v_o}{100 \text{ km s}^{-1}}\right] [X^*-X_f+\Phi] \tag{25}$$

To fit the radio spectrum with these equations, we need to determine the shock parameters. For HH1 and 2, we adopted the velocities of the condensations HH1F and HH2H (Herbig and Jones 1981), which are ~350 and ~240 km s^{-1}, respectively. Furthermore, we adopted as the angular diameter of HH1 and 2 those measured from the photographs of Herbig and Jones (1981), 3" and 4."4, respectively. Finally, if we adopt a magnetic field of ~90 µGauss (Cantó and Rodríguez 1986), we find that preshock densities of 85 cm^{-3} for HH1 and 200 cm^{-3} for HH2 give results that agree with the observed fluxes (see Table 1 and Figure 3).

Table 1. Observed and derived parameters for HH1, HH2 and the central source.

Source	n_o(cm^{-3})	v_o(km s^{-1})	Θ(arc sec)	λ(cm)	Flux (mJy) Observational[a]	Analytical
HH1	85	350	3	20	0.63	0.62
				6	0.55	0.55
				2	<0.54	0.49
HH2	200	240	4.4	20	1.50	1.36
				6	1.22	1.20
				2	0.83	1.08
CENTRAL	9.3x10^4	300	0.19	20	0.60	0.60
				6	1.20	1.65
				2	1.54	1.52

a) From Pravdo et al. (1985)

In the case of the central source there is no optical counterpart and the radio map of Pravdo et al. (1985) does not resolve the source. Correspondingly, we do not have an esti-- mate for its diameter. We will assume that the radio emission from this source comes from a shock wave produced by the interaction of a stellar wind with dense, surrounding gas, such as that forming a toroid (Torrelles et al. 1985). If we now assume that the 20 cm flux comes from the optically thick part of the spectrum, using equation (25) we derive an angular diameter of $0\overset{''}{.}19$ for the central source. Furthermore, assuming that the 2 cm flux is in the optically thin part of the spectrum and that $v_o \approx 300$ km s^{-1} (a typical value for T Tauri stars), we derive $n_o \approx 9.3 \times 10^4$ cm^{-3}. This density and velocity correspond to a mass loss rate of about 4.5×10^{-7} $M_\odot$ yr^{-1}, again a reasonable value. The spectrum obtained with these parameters is shown in Figure 3. As can be seen in this Figure, the observed spectra of HH1 and HH2 can be reproduced satisfactorily, while that of the central source is reproduced only partially. This discrepancy could be due to the radio emission of the central source not being produced by a plane-parallel shock wave, but by a different phenomenon such as an ionized stellar wind (Pravdo et al. 1985) or a combination of both phenomena.

CONCLUSIONS

Our main conclusions are:

The Hβ intensity from our analytical model varies approximately as v_o^2. This depen- dence and the intensity values are in good agreement with those obtained from the models of Ray- mond (1976,1979) and Shull and McKee (1979).

The thermal radio continuum produced by a shock wave is similar to that from photo- ionized regions. However, the numerical solution (that includes the contribution of the cooling zone and the recombination zone) suggests that significant differences appear in the optically thick part of the spectrum. These differences could allow a radio criterion to distinghish be- tween shock waves and photoionized regions.

Our analytical model can account satisfactorily for the radio observations of HH1 and 2. We derived the shock parameters for these sources. The radio spectrum of the central source cannot be reproduced with a plane-parallel shock wave. The emission from this source is probably produced by an ionized stellar wind or by a combination of stellar wind and shock wave phenomena.

REFERENCES

Abramowitz, M. and Stegun, I., 1972, *Handbook of Mathematical Functions, Dover Publications,Inc.*
Böhm, K. H., 1983. *Rev. Mexicana Astron. Astrof.*, 7, 55.
Cantó, J. and Rodríguez, L. F., 1986, *Rev. Mexicana Astron. Astrof.*, 13, 57.
Curiel, S., 1986. *B. S. Thesis, U.N.A.M.* México.
Dopita, M. A., 1978, *Ap. J. Suppl.*, 37, 117.
Haro, G., 1952, *Ap. J.*, 115, 572.
Hartmann, L. and Raymond, J. C., 1984, *Ap. J.*, 276, 560.
Herbig, G. H., 1951, *Ap. J.*, 113, 697.
Herbig, G. H. and Jones, B. F., 1981. *Ap. J.*, 86, 1232.
Mezger, P. G. and Henderson A. P., 1967, *Ap. J.*, 147, 471.
Osterbrock, D. E., 1974, *Astrophysics of Gaseous Nebula*, W. H. Freeman and Company, U. S. A.
Pravdo, S. H. Rodríguez, L. F., Curiel, S., Cantó, J., Torrelles, J. M., Becker, R. H. and
        Sellgren, K., 1985, *Ap. J. (Letters)*, 293, L35.
Panagia, N. and Felli, M., 1975, *Astron. Ap.*, 39, 1.
Raymond, J. C., 1976, *Ph. D. Thesis*, University of Wisconsin, Madison.
Raymond, J. C., 1979, *Ap. J. Suppl.*, 39, 1.
Shull, J. M. and McKee, C. F., 1979, *Ap. J.*, 227, 131.
Schwartz, R. D., 1978, *Ap. J.*, 223, 884.
Torrelles, J. M., Cantó, J., Rodríguez, L. F., Ho, P. T. P. and Moran, J. M., 1985, *Ap. J.
        (Letters)*, 294, L117.
Wright, A. E. and Barlow, M. J., 1975. *M.N.R.A.S.*, 170, 41.

Jorge Cantó, Salvador Curiel and Luis F. Rodríguez: Instituto de Astronomía, UNAM, Apartado
        Postal 70-264, 04510 México, D. F., México.